Proceedings of the ASME 2013 Dynamic Systems and Control Conference
DSCC2013
October 21-23, 2013, Palo Alto, California, USA

DSCC2013-3877

ADAPTIVE CONTROL WITH CONVEX SATURATION CONSTRAINTS

Jin Yan
Dept. of Aerospace Engineering
University of Michigan
Ann Arbor, MI 48109-2140
Email: yanjin@umich.edu

Davi Antônio dos Santos
Instituto Tecnolõgico de Aeronáutica
Divisão de Engenharia Mecânica-Aeronáutica
12228-900 São José dos Campos, SP, Brazil
Email: davists@ita.br

Dennis S. Bernstein *
Dept. of Aerospace Engineering
University of Michigan
Ann Arbor, MI 48109-2140
Email: dsbaero@umich.edu

ABSTRACT

This paper applies retrospective cost adaptive control (RCAC) to command following in the presence of multivariable convex input saturation constraints. To account for the saturation constraint, we use convex optimization to minimize the quadratic retrospective cost function. The use of convex optimization bounds the magnitude of the retrospectively optimized input and thereby influences the controller update to satisfy the control bounds. This technique is applied to a tiltrotor with constraints on the total thrust magnitude and inclination of the rotor plane.

1 Introduction

All real-world control systems must operate subject to constraints on the allowable control inputs. These constraints typically have the form of a saturation input nonlinearity [1]. The effects of saturation are traditionally addressed through anti-windup strategies [2, 3]. Within the context of modern multivariable control, techniques for dealing with saturation are presented in [4–7]. Saturation within the context of adaptive control is addressed in [8–10].

In the case of multiple control inputs, it is usually the case that individual control inputs are subject to independent saturation [11]. However, in many applications, a saturation constraint may constrain multiple control inputs. This is the case, for example, if the control inputs are produced by common hardware, such as a single power supply, amplifier, or actuator.

In the present paper we consider adaptive control for problems in which multiple control inputs may be subject to *dependent* saturation constraints. In particular, we are motivated by the problem of safely controlling the trajectory of a multi-rotor helicopter by constraining the total thrust magnitude and inclination in order to restrict the vehicle acceleration.

To address this problem, we revisit the problem of retrospective cost adaptive control (RCAC) under constraints [10]. RCAC can be used for adaptive command following and disturbance rejection for possibly nonminimum-phase systems under minimal modeling information [12–15]. Unlike [11], the present paper uses convex optimization to perform the retrospective input optimization [16]. The use of convex optimization bounds the magnitude of the retrospectively optimized input and thereby influences the controller update to satisfy the control bounds. We demonstrate this technique on illustrative numerical examples involving single and multiple inputs. We then apply this approach to trajectory control for a multi-rotor helicopter. We use the convex programming code [17] for the numerical optimization. A related technique was used within the context of RCAC in [18] to address the problem of unknown nonminimum-phase zeros.

The contents of the paper are as follows. In Section 2, we describe the command-following problem with input saturation nonlinearities. In Section 3, we summarize the RCAC algorithm. Numerical simulation results are presented in Section 4, and conclusions are given in Section 5.

2 Problem Formulation

Consider the MIMO discrete-time Hammerstein system

$$x(k+1) = Ax(k) + B\mathrm{Sat}(u(k)) + D_1 w(k), \tag{1}$$
$$y(k) = Cx(k) + D_2 w(k), \tag{2}$$
$$z(k) = E_1 x(k) + E_0 w(k), \tag{3}$$

*Address all correspondence to this author.

where, for all $k \geq 0$, $x(k) \in \mathbb{R}^n$, $y(k) \in \mathbb{R}^{l_y}$, $z(k) \in \mathbb{R}^{l_z}$, $w(k) \in \mathbb{R}^{l_w}$, and $u(k) \in \mathbb{R}^{l_u}$. The signal $u(k)$ is the commanded control input. However, due to saturation, the actual control input is given by $v(k) = \mathrm{Sat}(u(k))$, where the saturation input nonlinearity is $\mathrm{Sat} : \mathbb{R}^{l_u} \to \mathcal{U}$, and $\mathcal{U} \subseteq \mathbb{R}^{l_u}$ is the convex control constraint set. We assume that the function "Sat" is onto, that is, $\mathrm{Sat}(\mathbb{R}^{l_u}) = \mathcal{U}$. In particular, if $\mathcal{U}$ is rectangular, then

$$\mathrm{Sat}(u) = \begin{bmatrix} \mathrm{sat}_{a_1,b_1}(u_1) \\ \vdots \\ \mathrm{sat}_{a_{l_u},b_{l_u}}(u_{l_u}) \end{bmatrix}, \tag{4}$$

where $u = [u_1 \ \cdots \ u_{l_u}]^{\mathrm{T}} \in \mathcal{U} = [a_1, b_1] \times \cdots \times [a_{l_u}, b_{l_u}]$ and $\mathrm{sat} : \mathbb{R} \to [a, b]$ is defined as

$$\mathrm{sat}_{a,b}(u) = \begin{cases} a, & \text{if} \quad u < a, \\ u, & \text{if} \quad a \leq u \leq b, \\ b, & \text{if} \quad u > b. \end{cases} \tag{5}$$

The goal is to develop an adaptive output feedback controller that minimizes the command-following error z with minimal modeling information about the plant dynamics. Note that w can represent either a command signal to be followed, an external disturbance to be rejected, or both. For example, if $D_1 = 0$ and $E_0 \neq 0$, then the objective is to have the output $E_1 x$ follow the command signal $-E_0 w$. On the other hand, if $D_1 \neq 0$ and $E_0 = 0$, then the objective is to reject the disturbance w from the performance variable $E_1 x$. The combined command-following and disturbance-rejection problem is considered when $D_1 = \begin{bmatrix} D_{11} & 0 \end{bmatrix}$, $E_0 = \begin{bmatrix} 0 & E_{02} \end{bmatrix}$, and $w(k) = \begin{bmatrix} w_1^{\mathrm{T}}(k) & w_2^{\mathrm{T}}(k) \end{bmatrix}^{\mathrm{T}}$, where the objective is to have $E_1 x$ follow $-E_0 w_2$ while rejecting the disturbance w_1. Finally, if D_1 and E_0 are zero matrices, then the objective is output stabilization, that is, convergence of z to zero.

3 Retrospective Cost Adaptive Control

In this section, we describe the constrained retrospective cost optimization algorithm.

3.1 ARMAX Modeling

Consider the ARMAX representation of (1)–(3) given by

$$z(k) = \sum_{i=1}^{n} -\alpha_i z(k-i) + \sum_{i=d}^{n} \beta_i \mathrm{Sat}(u(k-i)) + \sum_{i=0}^{n} \gamma_i w(k-i), \tag{6}$$

where $\alpha_1, \ldots, \alpha_n \in \mathbb{R}$, $\beta_1, \ldots, \beta_n \in \mathbb{R}^{l_z \times l_u}$, $\gamma_0, \ldots, \gamma_n \in \mathbb{R}^{l_z \times l_w}$, and d is the relative degree. Next, let $v(k) \triangleq \mathrm{Sat}(u(k))$, and define the transfer function

$$G_{zv}(\mathbf{q}) \triangleq E_1(\mathbf{q}I - A)^{-1}B = \sum_{i=d}^{\infty} \mathbf{q}^{-i} H_i = H_d \frac{\alpha(\mathbf{q})}{\beta(\mathbf{q})}, \tag{7}$$

where $\mathbf{q}$ is the forward shift operator and, for each positive integer i, the Markov parameter H_i of G_{zv} is defined by

$$H_i \triangleq E_1 A^{i-1} B \in \mathbb{R}^{l_z \times l_u}. \tag{8}$$

Note that, if $d = 1$, then $H_1 = \beta_1$, whereas, if $d \geq 2$, then

$$\beta_1 = \cdots = \beta_{d-1} = H_1 = \cdots = H_{d-1} = 0 \tag{9}$$

and $H_d = \beta_d$. The polynomials $\alpha(\mathbf{q})$ and $\beta(\mathbf{q})$ have the form

$$\alpha(\mathbf{q}) = \mathbf{q}^{n-1} + \alpha_1 \mathbf{q}^{n-1} + \cdots + \alpha_{n-1}\mathbf{q} + \alpha_n, \tag{10}$$

$$\beta(\mathbf{q}) = \mathbf{q}^{n-d} + \beta_{d+1}\mathbf{q}^{n-d-1} + \cdots + \beta_{n-1}\mathbf{q} + \beta_n. \tag{11}$$

Next, define the *extended performance* $Z(k) \in \mathbb{R}^{pl_z}$ and *extended plant input* $V(k) \in \mathbb{R}^{q_c l_u}$ by

$$Z(k) \triangleq \begin{bmatrix} z(k) \\ \vdots \\ z(k-p+1) \end{bmatrix},$$

$$V(k) \triangleq \begin{bmatrix} v(k-1) \\ \vdots \\ v(k-q_c) \end{bmatrix} = \begin{bmatrix} \mathrm{Sat}(u(k-1)) \\ \vdots \\ \mathrm{Sat}(u(k-q_c)) \end{bmatrix}, \tag{12}$$

where the data window size p is a positive integer, and $q_c \triangleq n + p - 1$. Therefore (12) can be expressed as

$$Z(k) = W_{zw}\phi_{zw}(k) + B_f V(k), \tag{13}$$

where

$$W_{zw} \triangleq \begin{bmatrix} -\alpha_1 I_{l_z} & \cdots & -\alpha_n I_{l_z} & 0_{l_z \times l_z} & \cdots & 0_{l_z \times l_z} & \gamma_0 & \cdots & \gamma_n & 0_{l_z \times l_w} & \cdots & 0_{l_z \times l_w} \\ 0_{l_z \times l_z} & \ddots & & \ddots & \ddots & \vdots & 0_{l_z \times l_w} & \ddots & & \ddots & \ddots & \vdots \\ \vdots & \ddots & \ddots & & \ddots & 0_{l_z \times l_z} & \vdots & \ddots & \ddots & & \ddots & 0_{l_z \times l_w} \\ 0_{l_z \times l_z} & \cdots & 0_{l_z \times l_z} & -\alpha_1 I_{l_z} & \cdots & -\alpha_n I_{l_z} & 0_{l_z \times l_w} & \cdots & 0_{l_z \times l_w} & \gamma_0 & \cdots & \gamma_n \end{bmatrix}$$

$$\in \mathbb{R}^{pl_z \times [q_c l_z + (q_c+1) l_w]}, \tag{14}$$

$$
B_f \triangleq \begin{bmatrix} \beta_1 & \cdots & \beta_n & 0_{l_z\times l_u} & \cdots & 0_{l_z\times l_u} \\ 0_{l_z\times l_u} & \ddots & & \ddots & \ddots & \vdots \\ \vdots & \ddots & \ddots & & \ddots & 0_{l_z\times l_u} \\ 0_{l_z\times l_u} & \cdots & 0_{l_z\times l_u} & \beta_1 & \cdots & \beta_n \end{bmatrix} \in \mathbb{R}^{pl_z\times q_c l_u}, \tag{15}
$$

and

$$
\phi_{zw}(k) \triangleq \begin{bmatrix} z(k-1) \\ \vdots \\ z(k-p-n+1) \\ w(k) \\ \vdots \\ w(k-p-n+1) \end{bmatrix} \in \mathbb{R}^{q_c l_z+(q_c+1)l_w}. \tag{16}
$$

Note that W_{zw} includes modeling information about the poles of G_{zv} and the exogenous signals, while B_f includes modeling information about the zeros of G_{zv}.

3.2 Controller Construction

The commanded control $u(k)$ is given by the exactly proper time-series controller

$$
u(k) = \sum_{i=1}^{n_c} M_i(k)u(k-i) + \sum_{j=0}^{n_c} N_j(k)z(k-j), \tag{17}
$$

where, for all $i = 1,\ldots,n_c$, $M_i(k) \in \mathbb{R}^{l_u\times l_u}$, and, for all $j = 0,\ldots,n_c$, $N_j(k) \in \mathbb{R}^{l_u\times l_z}$. We express (17) as

$$
u(k) = \theta(k)\phi(k-1), \tag{18}
$$

where

$$
\theta(k) \triangleq \begin{bmatrix} M_1(k) & \cdots & M_{n_c}(k) & N_0(k) & \cdots & N_{n_c}(k) \end{bmatrix} \in \mathbb{R}^{l_u\times(n_c l_u+(n_c+1)l_z)} \tag{19}
$$

and

$$
\phi(k-1) \triangleq \begin{bmatrix} u(k-1) \\ \vdots \\ u(k-n_c) \\ z(k) \\ \vdots \\ z(k-n_c) \end{bmatrix} \in \mathbb{R}^{n_c l_u+(n_c+1)l_z}. \tag{20}
$$

3.3 Retrospective Performance

Define the *retrospective performance* $\hat{Z}(k) \in \mathbb{R}^{pl_z}$ by

$$
\hat{Z}(k) \triangleq W_{zw}\phi_{zw}(k) + B_f V(k) + \bar{B}_f[\hat{U}(k) - U(k)], \tag{21}
$$

where

$$
\bar{B}_f \triangleq \begin{bmatrix} 0_{l_z\times(d-1)l_u} & \bar{H}_d & \cdots & \bar{H}_m & 0_{l_z\times l_u} & \cdots & 0_{l_z\times l_u} & 0_{l_z\times l_u} & \cdots & 0_{l_z\times l_u} \\ 0_{l_z\times(d-1)l_u} & 0_{l_z\times l_u} & \ddots & & \ddots & \ddots & & \ddots & \ddots & \vdots \\ \vdots & \vdots & \ddots & \ddots & & \ddots & \ddots & & \ddots & \vdots \\ 0_{l_z\times(d-1)l_u} & 0_{l_z\times l_u} & \cdots & 0_{l_z\times l_u} & \bar{H}_d & \cdots & \bar{H}_m & 0_{l_z\times l_u} & \cdots & 0_{l_z\times l_u} \end{bmatrix} \in \mathbb{R}^{pl_z\times q_c l_u} \tag{22}
$$

is the *retrospective input matrix* with the model information of G_{zv}. Specifically, $\bar{H}_1,\ldots,\bar{H}_m$in (22) are estimates of the Markov parameters of G_{zv}, where $m \in \mathbb{Z}^+$. Next, define the *extended commanded control* $U(k) \in \mathbb{R}^{q_c l_u}$ and the *retrospectively optimized extended control vector* $\hat{U}(k) \in \mathbb{R}^{q_c l_u}$ by

$$
U(k) \triangleq \begin{bmatrix} u(k-1) \\ \vdots \\ u(k-q_c) \end{bmatrix}, \quad \hat{U}(k) \triangleq \begin{bmatrix} \hat{u}_k(k-1) \\ \vdots \\ \hat{u}_k(k-q_c) \end{bmatrix}, \tag{23}
$$

where $\hat{u}_k(k-i) \in \mathbb{R}^{l_u}$ is a recomputed control. Subtracting (13) from (21) yields

$$
\hat{Z}(k) = Z(k) + \bar{B}_f[\hat{U}(k) - U(k)]. \tag{24}
$$

Note that the retrospective performance $\hat{Z}(k)$ does not depend on W_{zw} or the exogenous signal w. For disturbance rejection, we do not assume that the disturbance is known; for command-following, the command-following error is needed but the command w need not be separately measured. The model information matrix $\bar{B}_f$ is discussed in Section 3.5.

3.4 Retrospective Cost and RLS Controller Update Law

3.4.1 Retrospective Cost We define the *retrospective cost function*

$$
J(\hat{U}(k),k) \triangleq \hat{Z}^{\mathrm{T}}(k)R(k)\hat{Z}(k) + \eta(k)\hat{U}(k)^{\mathrm{T}}\hat{U}(k), \tag{25}
$$

where, for all $k > 0$, $\eta(k) \geq 0$ is a scalar and $R(k) \in \mathbb{R}^{pl_z\times pl_z}$ is a positive-definite performance weighting. The goal is to determine retrospectively optimized controls $\hat{U}(k)$ that would have provided better performance than the controls $U(k)$ that were applied to the plant. The retrospectively optimized controls $\hat{U}(k)$ are subsequently used to update the controller. Using (24), (25) can be rewritten as

$$J(\hat{U}(k),k) = \hat{U}(k)^{\mathrm{T}}\mathcal{A}(k)\hat{U}(k) + \mathcal{B}(k)\hat{U}(k) + \mathcal{C}(k), \tag{26}$$

where

$$\mathcal{A}(k) \stackrel{\triangle}{=} \bar{B}_f^{\mathrm{T}} R(k)\bar{B}_f + \eta(k) I_{q_c l_u},$$
$$\mathcal{B}(k) \stackrel{\triangle}{=} 2\bar{B}_f^{\mathrm{T}} R(k)[Z(k) - \bar{B}_f U(k)],$$
$$\mathcal{C}(k) \stackrel{\triangle}{=} Z^{\mathrm{T}}(k)R(k)Z(k) - 2Z^{\mathrm{T}}(k)R(k)\bar{B}_f U(k) + U(k)^{\mathrm{T}}\bar{B}_f^{\mathrm{T}} R(k)\bar{B}_f U(k).$$

Note that if either $\bar{B}_f$ has full rank or $\eta(k) > 0$, then $\mathcal{A}(k)$ is positive definite.

Next, we consider the problem of minimizing (25) subject to

$$\hat{U}(k) \in \mathcal{U} \times \cdots \times \mathcal{U}. \tag{27}$$

3.4.2 Cumulative Cost and RLS Update

Define the *cumulative cost function*

$$J_{\mathrm{cum}}(\theta,k) \stackrel{\triangle}{=} \sum_{i=d+1}^{k} \lambda^{k-i} \|\phi^{\mathrm{T}}(i-d-1)\theta(i-1) - \hat{u}_k(i-d)\|^2 + \lambda^k [\theta(k) - \theta(0)]^{\mathrm{T}} P_0^{-1} [\theta(k) - \theta(0)], \tag{28}$$

where $\|\cdot\|$ is the Euclidean norm, $P_0 \in \mathbb{R}^{l_u[n_c l_u + (n_c+1)l_z] \times [n_c l_u + (n_c+1)l_z]}$ is positive definite, and $\lambda \in (0,1]$ is the forgetting factor. The next result follows from standard recursive least-squares (RLS) theory [19, 20].

Lemma 3.1. *For each $k \geq d$, the unique global minimizer of the cumulative retrospective cost function* (28) *is given by*

$$\theta(k) = \theta(k-1) + \frac{P(k-1)\phi(k-d)\varepsilon(k-1)}{\lambda + \phi^{\mathrm{T}}(k-d)P(k-1)\phi(k-d)}, \tag{29}$$

where

$$P(k) = \frac{1}{\lambda}\left[P(k-1) - \frac{P(k-1)\phi(k-d)\phi^{\mathrm{T}}(k-d)P(k-1)}{\lambda + \phi^{\mathrm{T}}(k-d)P(k-1)\phi(k-d)}\right], \tag{30}$$

$P(0) = P_0$, and $\varepsilon(k-1) \stackrel{\triangle}{=} \phi^{\mathrm{T}}(k-d-1)\theta(k-1) - \hat{u}(k-d)$.

3.5 Model Information $\bar{B}_f$

For SISO, minimum-phase, asymptotically stable linear plants, using the first nonzero Markov parameter in $\bar{B}_f$ yields asymptotic convergence of z to zero [13, 21]. In this case, let $m = d$ and $\bar{H}_d = H_d$ in (22). Furthermore, if the open-loop linear plant is nonminimum-phase and the absolute values of all nonminimum-phase zeros are greater than the plant's spectral radius, then a sufficient number of Markov parameters can be used to approximate the nonminimum-phase zeros [13]. Alternatively, a phase-matching condition with $\eta > 0$ is given in [22, 23] to construct $\bar{B}_f$. For MIMO Lyapunov-stable linear plants, an extension of the phase-matching-based method is given in [24]. For unstable, nonminimum-phase plants, knowledge of the locations of the nonminimum-phase zeros is needed to construct $\bar{B}_f$. For details, see [13, 25].

In this paper, we consider only the case where the zeros of G_{zv} are either minimum-phase or on the unit circle. Therefore, we set $p = 1$ and let $\bar{B}_f = \begin{bmatrix} 0_{1_z \times (d-1)l_u} & H_d & 0_{1_z \times (n-d)l_u} \end{bmatrix} \in \mathbb{R}^{l_z \times n l_u}$.

4 Numerical Examples

In this section, we present numerical examples to illustrate the response of RCAC for plants with input saturation based on constrained retrospective optimization. The numerical examples are constructed such that the objective is to minimize the performance $z = y - w$, with $\phi(k)$ given by (20). In all simulations, we set $\lambda = 1$ and initialize $\theta(0)$ to zero.

Example 4.1. *Step command following for mass-spring-damper structure with single-direction force actuation.* Consider the mass-spring-damper structure shown in Figure 1 modeled by equation (31)

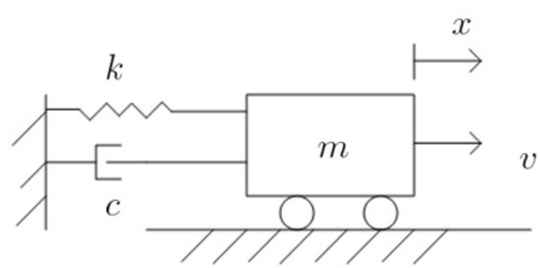

Figure 1. Example 4.1. Mass-spring-damper structure with single-direction force actuation.

$$m\ddot{x} + c\dot{x} + kx = v, \tag{31}$$

where m, c, k are the mass, damping, and stiffness, respectively,

w is the command signal, and v is the force input given by

$$v = \mathrm{sat}(u) = \begin{cases} u & \text{if} \quad u \geq 0, \\ 0 & \text{otherwise.} \end{cases} \tag{32}$$

Next, the state space representation of the mass-spring-damper structure can be written as

$$\begin{bmatrix} \dot{x} \\ \ddot{x} \end{bmatrix} = \begin{bmatrix} 0 & 1 \\ -\frac{k}{m} & -\frac{c}{m} \end{bmatrix} \begin{bmatrix} x \\ \dot{x} \end{bmatrix} + \begin{bmatrix} 0 \\ \frac{1}{m} \end{bmatrix} v, \tag{33}$$

$$y = \begin{bmatrix} 0 & 1 \end{bmatrix} \begin{bmatrix} x \\ \dot{x} \end{bmatrix}, \tag{34}$$

$$z = x - w, \tag{35}$$

where x and $\dot{x}$ are the position and velocity, respectively, of the mass. We discretize (33)-(35) using zero-order-hold and the plant transfer function from v to z, given by

$$G_{zv}(\mathbf{z}) = \frac{0.004(\mathbf{z}+0.85)}{\mathbf{z}^2 - 1.38\mathbf{z} + 0.61}. \tag{36}$$

Our goal is to have the plant output y follow the step command $w(k)$. We consider the saturation where the input to the plant $v = \mathrm{sat}(u)$ is given by (5). Specifically, we let $v^{\min} = 0$ and $v^{\max} = \infty$ when we compute the retrospectively optimized control $\hat{u}(k)$ in (27). The adaptive controller (17) with known saturation bounds is implemented in feedback with $n_c = 5$, $\eta = 0.01$, $P_0 = 0.01I$, and $B_f = 0.004$. Note that, $v^{\min}$, $v^{\max}$, and $\bar{B}_f$ are the only required model information for the adaptive controller. Furthermore, we initialize the adaptive controller gain matrix $\theta(0)$ to zero.

Figure 2 shows the time history of w, y, u, and v for the case where $v^{\min} = 0$ and $v^{\max} = \infty$ in (5). The adaptive controller is able to follow the step commands with single-direction force actuation. In particular, by an appropriate modification of the retrospectively optimized control $\hat{u}(k)$, excessive adaptation of the unsaturated control signal u is prevented, that is, $u(k) \geq 0$ for all k.

This problem is closely related to the classical problem of controllability using positive controls considered in [26–28]. However, Brammers theorem given in [26, 27] assumes that $B = I$, which is not the case in this example.

Example 4.2. *Square wave command following for a minimum-phase, asymptotically stable plant with saturation*
Consider the asymptotically stable, minimum-phase plant trans-

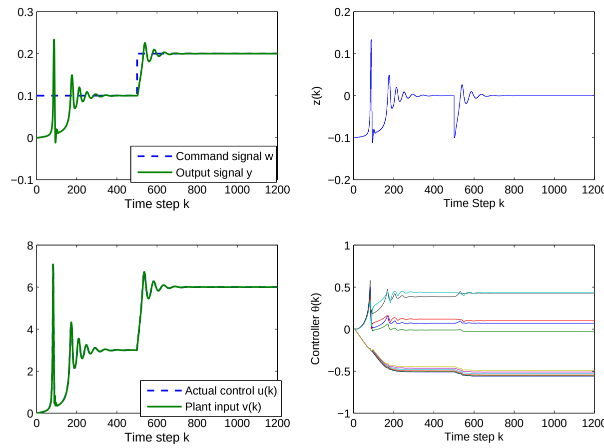

Figure 2. Example 4.1. *Step command following for mass-spring-damper structure with single-direction force actuation.* We consider the saturation constraints where the input to the plant $v = \mathrm{sat}(u)$ is given by (5). Specifically, we let $v^{\min} = 0$ and $v^{\max} = \infty$ when we compute the retrospectively optimized control $\hat{u}(k)$ in (27). The adaptive controller (17) with known saturation bounds is implemented in feedback with $n_c = 5$, $\eta = 0.01$, $P_0 = 0.01I$, and $B_f = 0.004$. Note that $v^{\min}$, $v^{\max}$, and $\bar{B}_f$ are the only required model information for the adaptive controller. Furthermore, we initialize the adaptive controller gain matrix $\theta(0)$ to zero. The adaptive controller is able to follow the step commands with one-direction force actuator input. In particular, by an appropriate modification of the retrospectively optimized control $\hat{u}(k)$, excessive adaptation of the unsaturated control signal u is prevented, that is, $u(k) \geq 0$ for all k.

fer function from v to z, given by

$$G_{zv}(\mathbf{z}) = \frac{(\mathbf{z}-0.5)(\mathbf{z}-0.9)}{(\mathbf{z}-0.7)(\mathbf{z}-0.5-j0.5)(\mathbf{z}-0.5+j0.5)}. \tag{37}$$

Our goal is to have the plant output y follow the square-wave command $w(k) = w_{\mathrm{s}}(k)$. We consider the unsaturated case, that is, $v^{\min} = -\infty$ and $v^{\max} = \infty$, together with four levels of saturation. Let $u_{\mathrm{ss,max}} = 3$ and $u_{\mathrm{ss,min}} = -3$ be maximum and minimum steady-state command values that drive the performance z to zero in steady-state (i.e. $z_{\mathrm{ss}} = 0$), respectively. Next, we define four saturation levels, specifically, $v^{\max,10\%} = 0.9u_{\mathrm{ss,max}}$, $v^{\max,20\%} = 0.8u_{\mathrm{ss,max}}$, $v^{\max,40\%} = 0.6u_{\mathrm{ss,max}}$, $v^{\max,80\%} = 0.2u_{\mathrm{ss,max}}$, $v^{\min,10\%} = 0.9u_{\mathrm{ss,min}}$, $v^{\min,20\%} = 0.8u_{\mathrm{ss,min}}$, $v^{\min,40\%} = 0.6u_{\mathrm{ss,min}}$, and $v^{\min,80\%} = 0.2u_{\mathrm{ss,min}}$. In all the four cases, the adaptive controller (17) with known saturation bounds in (27) is implemented in feedback with $n_c = 3$, $\eta = 0$, $P_0 = 10^{-2}I$, and $B_f = 1$. Note that, $v^{\min}$, $v^{\max}$, and $\bar{B}_f$ are the only required model information for the adaptive controller. Furthermore, the adaptive controller gain matrix $\theta(0)$ is initialized to zero. That is, no baseline controller is used to initialize RCAC.

Figure 3 shows the time history of w, y, u, and v for the case without saturation as well as the case where the control output u has 10%, 20%, 40%, and 80% saturation. For the case without saturation, y follows the command w with zero steady-state error. For the case with saturation, note that the adaptive controller is not able to follow the commands with zero steady-state error because the saturation makes this impossible. However, the unsaturated control signal u does not exhibit integrator windup, and the output y is able to match w without phase lag.

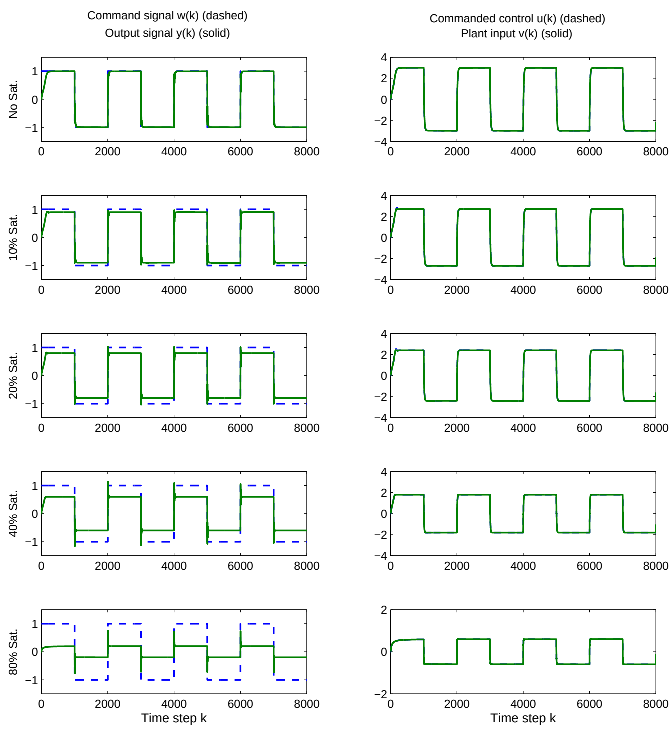

Figure 3. Example 4.2. *Square wave command following for a minimum-phase, asymptotically stable plant with saturation.* The adaptive controller (17) is implemented in feedback with $n_c = 3, \eta = 0$, $P_0 = 10^{-2}I$, and $\bar{B}_f = 1$. Note that, $v^{\min}$, $v^{\max}$, and $\bar{B}_f$ are the only required model information for the adaptive controller. The adaptive controller gain matrix $\theta(0)$ is initialized to zero. We consider the case without saturation as well as the case where the control output u has 10%, 20%, 40%, and 80% saturation. For the case without saturation, y follows the command w with zero steady-state error. For the case with saturation, note that the adaptive controller is not able to follow the commands with zero steady-state error because the saturation makes this impossible. However, the unsaturated control signal u does not exhibit integrator windup, and the output y is able to match w without phase lag.

Example 4.3. *Triangle wave command following for a minimum-phase, Lyapunov stable plant with saturation*
Consider the Lyapunov stable, minimum-phase plant transfer function from v to z, given by

$$G_{zv}(\mathbf{z}) = \frac{1}{\mathbf{z}-1}. \tag{38}$$

Our goal is to have the plant output y follow the triangle-wave command $w(k) = w_{\rm t}(k)$. We consider the unsaturated case, that is, $v^{\min} = -\infty$ and $v^{\max} = \infty$, together with four levels of saturation. Let $u_{\rm ss,max}$ and $u_{\rm ss,min}$ be maximum and minimum steady-state command values that drive the performance z to zero in steady-state (i.e. $z_{\rm ss} = 0$), respectively. Next, we define four saturation levels, specifically, $v^{\max,10\%} = 0.9u_{\rm ss,max}$, $v^{\max,20\%} = 0.8u_{\rm ss,max}$, $v^{\max,40\%} = 0.6u_{\rm ss,max}$, $v^{\max,80\%} = 0.2u_{\rm ss,max}$, $v^{\min,10\%} = 0.9u_{\rm ss,min}$, $v^{\min,20\%} = 0.8u_{\rm ss,min}$, $v^{\min,40\%} = 0.6u_{\rm ss,min}$, and $v^{\min,80\%} = 0.2u_{\rm ss,min}$. In all the four cases, the adaptive controller (17) with known saturation bounds in (27) is implemented in feedback with $n_c = 3$, $\eta = 0$, $P_0 = 10^{-2}I$, and $B_f = 1$. Note that, $v^{\min}$, $v^{\max}$, and $\bar{B}_f$ are the only required model information for the adaptive controller. Furthermore, the adaptive controller gain matrix $\theta(0)$ is initialized to zero. That is, no baseline controller is used to initialize RCAC.

Figure 4 shows the time history of w, y, u, and v for the case without saturation as well as the case where the control output u has 10%, 20%, 40%, and 80% saturation. For the case without saturation, y follows the command w. Each time the slope of w changes sign, the control u experiences a transient. This is because RCAC adapts itself to follow the new command and the output $y(k)$ reaches zero steady-state error. For the case with saturation, note that the adaptive controller is not able to follow the commands with zero steady-state error because the saturation makes this impossible. However, the unsaturated control signal u does not exhibit integrator windup and remains bounded. In particular, the closed-loop system maintains stability.

Example 4.4. *Command following for a multi-rotor helicopter.* The translational motion of a multi-rotor helicopter is described by

$$\ddot{q} = \frac{1}{m}u + \begin{bmatrix} 0 \\ 0 \\ -g \end{bmatrix}, \tag{39}$$

where $q = \begin{bmatrix} q_1 & q_2 & q_3 \end{bmatrix}^{\rm T} \in \mathbb{R}^3$ denotes the position of the vehicle center of mass resolved in the Earth frame, where q_1 and q_2 denote horizontal displacements, while q_3 denotes the vertical displacement. The initial conditions are $q(0) = \begin{bmatrix} 0 & 0 & 0 \end{bmatrix}^{\rm T}$ and $\dot{q}(0) = \begin{bmatrix} 0 & 0 & 0 \end{bmatrix}^{\rm T}$. $u = \begin{bmatrix} u_1 & u_2 & u_3 \end{bmatrix}^{\rm T} \in \mathbb{R}^3$ is the control force, $g = 9.8$ m/s^2 is the gravitational acceleration, and $m = 0.5$ kg is the mass of the vehicle.

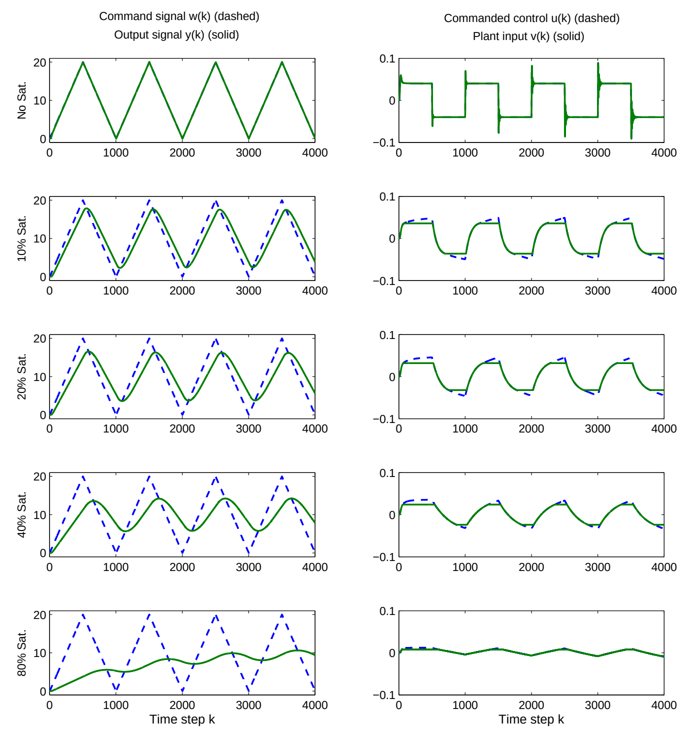

Figure 4. Example 4.3. *Triangle wave command following for a minimum-phase, Lyapunov stable plant with saturation.* The adaptive controller (17) is implemented in feedback with $n_c = 3, \eta = 0$, $P_0 = 10^{-2}I$, and $\bar{B}_f = 1$. Note that, $v^{\min}$, $v^{\max}$, and $\bar{B}_f$ are the only required model information for the adaptive controller. The adaptive controller gain matrix $\theta(0)$ is initialized to zero. We consider the case without saturation as well as the case where the control output u has 10%, 20%, 40%, and 80% saturation. For the case without saturation, y follows the command w. Each time the slope of w changes sign, the control u experiences a transient and the output $y(k)$ reaches zero steady-state error. For the case with saturation, note that the adaptive controller is not able to follow the commands with zero steady-state error because the saturation makes this impossible. However, the unsaturated control signal u does not exhibit integrator windup and remains bounded

Define the inclination angle φ of u to be

$$\varphi \triangleq \cos^{-1} \frac{u_3}{\|u\|}, \tag{40}$$

where $\|u\|$ denotes the Euclidean norm of u. Let

$$w(t) = \begin{bmatrix} 2\cos(0.1t) \\ 2\sin(0.1)t \\ 0.3t+1 \end{bmatrix} \in \mathbb{R}^3 \tag{41}$$

denote the position command, and define the tracking error $z \in \mathbb{R}^3$ by

$$z \triangleq q - w. \tag{42}$$

Let the positive real numbers $\varphi_{\max} = 20$ deg and $u_{\max} = 6$ N denote the maximum allowable values of φ and $\|u\|$, respectively. The control problem is thus to construct a feedback control law for u that minimizes $\|z\|$ subject to

$$\frac{\sqrt{u_1^2 + u_2^2}}{\|u\|} \le \sin\varphi_{\max}, \tag{43}$$

$$u_3 \ge 0, \tag{44}$$

and

$$\|u\| \le u_{\max}, \tag{45}$$

where (43)-(45) form the convex control constraint set $\mathcal{U}$ shown in Figure 5. The problem of minimizing the retrospective cost function on $\mathcal{U}$ can thus be rewritten as the following second-order cone programming (SOCP) problem:

$$\min J(\hat{U}(k), k) \tag{46}$$

subject to

$$\|P\hat{U}(k)\|_2 \le Q\hat{U}(k) \quad \text{and} \quad \|\hat{U}(k)\|_2 \le 6, \tag{47}$$

where $P \triangleq \begin{bmatrix} 1 & 0 & 0 \\ 0 & 1 & 0 \\ 0 & 0 & 0 \end{bmatrix}$ and $Q \triangleq \tan(\varphi_{\max}) \begin{bmatrix} 0 & 0 & 1 \end{bmatrix}^{\mathrm{T}}$. The nonlinear programming method SOCP in the CVX toolbox [17] is used to solve the optimization problem (46) and (47).

Next, a state space representation of the multi-rotor heli-

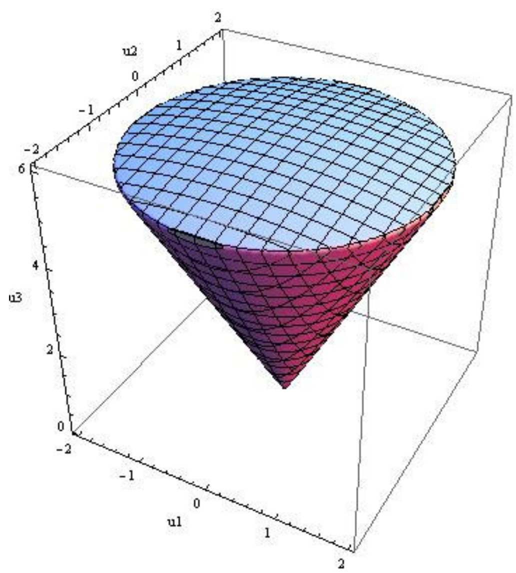

Figure 5. Example 4.4. The convex control constraint set $\mathcal{U}$ formed by (43)-(45).

copter is given by

$$\begin{bmatrix} \dot{q} \\ \ddot{q} \end{bmatrix} = \begin{bmatrix} 0_{3\times3} & I_{3\times3} \\ 0_{3\times3} & 0_{3\times3} \end{bmatrix} \begin{bmatrix} q \\ \dot{q} \end{bmatrix} + \begin{bmatrix} 0_{3\times3} \\ \frac{1}{m} I_{3\times3} \end{bmatrix} v + \begin{bmatrix} 0_{3\times1} \\ \begin{bmatrix} 0 \\ 0 \\ -g \end{bmatrix} \end{bmatrix}, \quad (48)$$

$$y = \begin{bmatrix} I_{3\times3} & 0_{3\times3} \end{bmatrix} \begin{bmatrix} q \\ \dot{q} \end{bmatrix}, \quad (49)$$

$$z = y - w, \quad (50)$$

where $v = \mathrm{Sat}(u) \in \mathcal{U}$ is the saturated control input given by

$$v = \begin{bmatrix} v_1 \\ v_2 \\ v_3 \end{bmatrix} = \mathrm{Sat}(u) = \begin{bmatrix} \mathrm{Sat}_1(u_1, u_2, u_3) \\ \mathrm{Sat}_2(u_1, u_2, u_3) \\ \mathrm{Sat}_3(u_3) \end{bmatrix}, \quad (51)$$

where

$$\mathrm{Sat}_1(u_1, u_2, u_3) \stackrel{\triangle}{=} \begin{cases} u_1 & \text{if} \quad u_1 \le \mathrm{Sat}_3(u_3) \tan \varphi_{\max} \cos \vartheta, \\ \mathrm{Sat}_3(u_3) \tan \varphi_{\max} \cos \vartheta & \text{otherwise}, \end{cases} \quad (52)$$

$$\mathrm{Sat}_2(u_1, u_2, u_3) \stackrel{\triangle}{=} \begin{cases} u_2 & \text{if} \quad u_2 \le \mathrm{Sat}_3(u_3) \tan \varphi_{\max} \sin \vartheta, \\ \mathrm{Sat}_3(u_3) \tan \varphi_{\max} \sin \vartheta & \text{otherwise}, \end{cases} \quad (53)$$

$$\mathrm{Sat}_3(u_3) \stackrel{\triangle}{=} \mathrm{sat}_{0,6}(u_3), \quad (54)$$

and

$$\vartheta \stackrel{\triangle}{=} \mathrm{atan2}(u_2, u_1) = 2 \arctan \frac{u_2}{\sqrt{u_1^2 + u_2^2} + u_1}. \quad (55)$$

Next, we discretize (48)-(50) using zero-order-hold. The adaptive controller (17) with knowledge of the saturation (47) is implemented in feedback with $n_c = 8$, $\eta = 0$, $P_0 = 0.1I$, $d = 1$, $H_1 = I_{3\times3}$, and we let $\bar{B}_f = \begin{bmatrix} 0.01 I_{3\times3} & 0_{3\times3} \end{bmatrix}$.

Figure 6 shows the time history of y_1, y_2, and y_3 of the helicopter. The transient especially along y_3 direction is due to the fact that (48)-(50) is unstable, the discretized equivalent of (48)-(50) has nonminimum-phase zeros at -1, and the gravitational acceleration g is unmodeled. Furthermore, we initialize the adaptive controller at $\theta(0) = 0$. Note that the commanded control signal u does not exhibit integrator windup and remains bounded as shown in Figure 7, where the black dots represent the control constraint set $\mathcal{U}$, and the blue crosses represent the commanded control u. Note that the blue crosses outside the control constraint set $\mathcal{U}$ (black dots region) are caused by the transient behavior of RLS update in (29) and (30). Figure 8 shows the distance between the unsaturated commanded control $u(k)$ (blue crosses that are outside the control constraint set $\mathcal{U}$ in Figure 7) and the saturated control $v(k)$ at each time step. ■

5 Conclusion

Adaptive control based on constrained retrospective cost optimization was applied to command following for Hammerstein systems with input saturation We numerically demonstrated that RCAC can improve the tracking performance when following square-wave and triangle-wave commands in the presence of saturation, provided that the saturation boundary is known. RCAC was used with limited modeling information. In particular, RCAC uses knowledge of the first nonzero Markov parameter of the linear system and the saturation bounds. We also applied this technique to a multi-rotor helicopter command-following problem by formulating the multi-input constrained retrospective cost function as a second-order cone optimization (SOCP) problem. With this approach, RCAC is shown to adapt to these constraints. Future research will include a stability analysis of RCAC under saturation input nonlinearity.

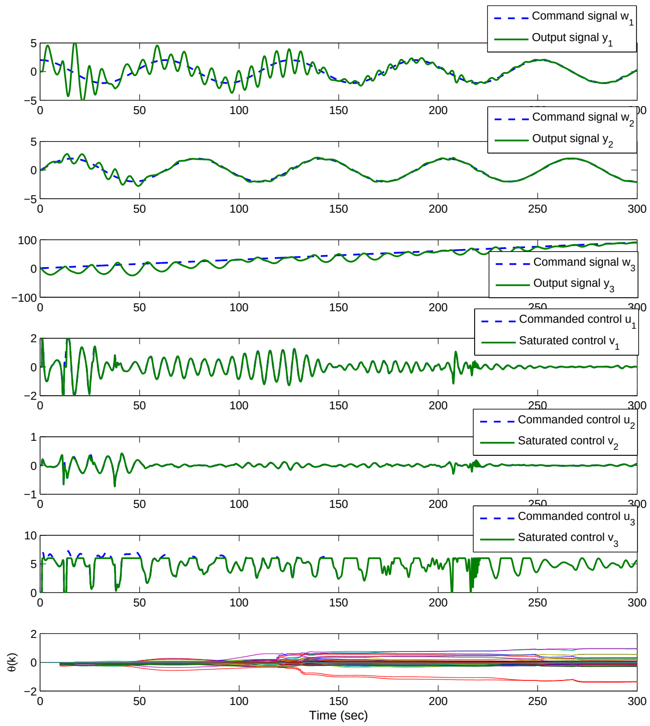

Figure 6. Example 4.4. *Command following for a multi-rotor helicopter.* The adaptive controller (17) with the saturation bounds in (47) is implemented in feedback with $n_c = 8$, $\eta = 0$, $P_0 = 0.1I$, $\bar{B}_f = [0.01I_{3\times3}\ 0_{3\times3}]$, and $\theta(0) = 0$. Note that the outputs of y_1, y_2, y_3 follow the commands w_1, w_2, and w_3 after the transient.

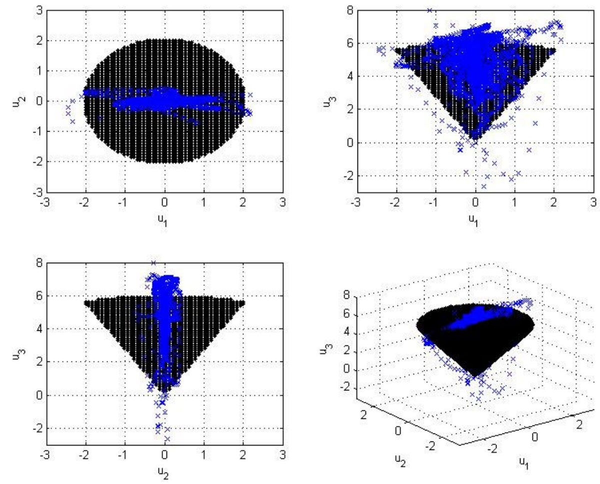

Figure 7. Example 4.4. The adaptive controller (17) with known saturation bounds in (47) is implemented in feedback with $n_c = 8$, $\eta = 0$, $P_0 = 0.1I$, $\bar{B}_f = [0.01I_{3\times3}\ 0_{3\times3}]$, and $\theta(0) = 0$. The black dots represent the constraint set in (43) and (45), and the blue dots represent the unsaturated controller output u. The blue crosses outside the boundary of the constraint (black dots region) are due to the transient behavior of RLS update in (29) and (30).

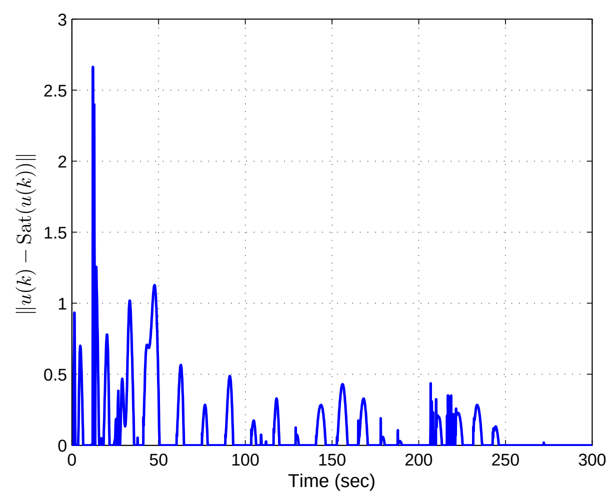

Figure 8. Example 4.4. At each time step, the distance between the unsaturated commanded control $u(k)$ (blue crosses that are outside the control constraint set $\mathcal{U}$ in Figure 7) and the saturated control $\mathrm{Sat}(u(k))$.

ACKNOWLEDGMENT

We wish to thank Jesse Hoagg and Alexey Morozov for helpful discussions.

REFERENCES

[1] Bernstein, D. S., and Michel, A. N., 1995. "A chronological bibliography on saturating actuators". *Int. J. Robust and Nonlinear Control,* **5**, pp. 375–380.

[2] Zaccarian, L., and Teel, A. R., 2011. *Modern Anti-windup Synthesis: Control Augmentation for Actuator Saturation*. Princeton University Press.

[3] Hippe, P., 2006. *Windup in Control: Its Effects and Their Prevention*. Springer.

[4] Hu, T., and Lin, Z., 2001. *Control Systems with Actuator Saturation: Analysis and Design*. Birkhäuser.

[5] Glattfelder, A., and Schaufelberger, W., 2003. *Control Systems with Input and Output Constraints*. Springer.

[6] Kapila, T., and Grigoriadis, K., 2002. *Actuator Saturation Control*. CRC Press.

[7] Tarbouriech, S., Garcia, G., da Silva Jr., J. M. G., and Queinnec, I., 2011. *Stability and Stabilization of Linear Systems with Saturating Actuators*. Springer.

[8] Annaswamy, A. M., and Wong, J.-E., 1998. "Adaptive control in the presence of saturation non-linearity". *Int. J. Adaptive Contr. Sig. Proc.,* **11**, pp. 3–19.

[9] Teo, J., and How, J. P., 2009. "Anti-windup compensation for nonlinear systems via gradient projection: Application to adaptive control". In Proc. IEEE Conf. Dec. Contr., pp. 6910–6916.

[10] Coffer, B. J., Hoagg, J. B., and Bernstein, D. S., 2011. "Cu-

mulative retrospective cost adaptive control of systems with amplitude and rate saturation". In Proc. Amer. Contr. Conf., pp. 2344–2349.

[11] Tyan, F., and Bernstein, D. S., 1999. "Global stabilization of systems containing a double integrator using a saturated linear controller". *Int. J. Robust Nonlinear Control,* **9**(15), pp. 1143–1156.

[12] Hoagg, J. B., Santillo, M. A., and Bernstein, D. S., 2008. "Discrete-time adaptive command following and disturbance rejection for minimum phase systems with unknown exogenous dynamics". *IEEE Trans. Autom. Contr.,* **53**, pp. 912–928.

[13] Santillo, M. A., and Bernstein, D. S., 2010. "Adaptive control based on retrospective cost optimization". *AIAA J. Guid. Contr. Dyn.,* **33**, pp. 289–304.

[14] Hoagg, J. B., and Bernstein, D. S., 2012. "Retrospective cost model reference adaptive control for nonminimum-phase systems". *AIAA J. Guid. Contr. Dyn.,* **35**, pp. 1767–1786.

[15] Hoagg, J. B., and Bernstein, D. S., 2010. "Retrospective cost adaptive control for nonminimum-phase discrete-time systems part 1: The ideal controller and error system; part 2: The adaptive controller and stability analysis". In Proc. IEEE Conf. Dec. Contr., pp. 893–904.

[16] D'Amato, A. M., and Bernstein, D. S., 2012. "Adaptive forward-propagating input reconstruction for nonminimum-phase systems". In Proc. Amer. Contr. Conf., pp. 598–603.

[17] Grant, M., and Boyd, S., 2013. CVX: Matlab software for disciplined convex programming, version 2.0. `http://cvxr.com/cvx/`, March.

[18] Morozov, A., D'Amato, A. M., Hoagg, J. B., and Bernstein, D. S., 2011. "Retrospective cost adaptive control for nonminimum-phase systems with uncertain nonminimum-phase zeros using convex optimization". In Proc. Amer. Contr. Conf., pp. 1188–2293.

[19] Åström, K. J., and Wittenmark, B., 1995. *Adaptive Control*. Addison-Wesley.

[20] Goodwin, G. C., and Sin, K. S., 1984. *Adaptive Filtering, Prediction, and Control*. Prentice Hall.

[21] D'Amato, A. M., Sumer, E. D., and Bernstein, D. S., 2011. "Frequency-domain stability analysis of retrospective-cost adaptive control for systems with unknown nonminimum-phase zeros". In Proc. IEEE Conf. Dec. Contr., pp. 1098–1103.

[22] Sumer, E. D., D'Amato, A. M., Morozov, A. M., Hoagg, J. B., and Bernstein, D. S., 2011. "Robustness of retrospective cost adaptive control to Markov-parameter uncertainty". In Proc. IEEE Conf. Dec. Contr., pp. 6085–6090.

[23] Sumer, E. D., Holzel, M. H., D'Amato, A. M., and Bernstein, D. S., 2012. "FIR-based phase matching for robust retrospective-cost adaptive control". In Proc. Amer. Contr. Conf., pp. 2707–2712.

[24] Sumer, E. D., and Bernstein, D. S., 2012. "Retrospective cost adaptive control with error-dependent regularization for mimo systems with unknown nonminimum-phase transmission zeros". In Proc. AIAA Guid. Nav. Contr. Conf. AIAA-2012-4070.

[25] Hoagg, J. B., and Bernstein, D. S., 2010. "Cumulative retrospective cost adaptive control with rls-based optimization". In Proc. Amer. Contr. Conf., pp. 4016–4021.

[26] Brammer, R. F., 1972. "Controllability in linear autonomous systems with positive controllers". *SIAM J. Control,* **10**, pp. 339–353.

[27] Jacobson, D. H., Margin, D. H., Pachter, M., and Geveci, T., 1980. *Extensions of Linear-Quadratic Control Theory*. Springer.

[28] Leyva, H., Sols-Daun, J., and Suárez, R., 2013. "Global CLF stabilization of systems with control inputs constrained to a hyperbox". *SIAM J. Control Optim.,* **51**, pp. 745–766.